International Journal of Particle Therapy 12 (2024) 100100

Contents lists available at ScienceDirect

International Journal of Particle Therapy

journal homepage: www.sciencedirect.com/journal/ijpt

Dosimetric Comparison Between Proton and Photon Radiation Therapies for Pediatric Neuroblastoma

Alfredo Mirandola[1,*,#], Francesca Colombo[2], Francesca Cavagnetto[3], Anna Cavallo[4], Marco Gusinu[3], Silvia Molinelli[1], Emanuele Pignoli[4], Mario Ciocca[1], Salvina Barra[5], Flavio Giannelli[5], Emilia Pecori[6], Barbara A. Jereczek-Fossa[7,8], Ester Orlandi[2,9], Sabina Vennarini[6]

[1] *Medical Physics Unit, National Center for Oncological Hadrontherapy, Pavia, Italy*
[2] *Radiotherapy Department, National Center for Oncological Hadrontherapy, Pavia, Italy*
[3] *Medical Physics Unit, IRCCS Ospedale Policlinico San Martino, Genoa, Italy*
[4] *Medical Physics Unit, Fondazione IRCCS Istituto Nazionale dei Tumori di Milano, Milan, Italy*
[5] *Radiation Oncology Department, IRCCS Ospedale Policlinico San Martino, Genoa, Italy*
[6] *Pediatric Radiotherapy Unit, Fondazione IRCCS Istituto Nazionale Tumori, Milan, Italy*
[7] *Division of Radiation Oncology, European Institute of Oncology IRCCS, Milan, Italy*
[8] *Department of Oncology and Hemato-Oncology, University of Milan, Milan, Italy*
[9] *Department of Clinical, Surgical, Diagnostic and Pediatric Services, University of Pavia, Pavia, Italy*

ARTICLE INFO

Keywords:
Neuroblastoma
Pediatric
Proton therapy
Plan comparison

ABSTRACT

Purpose: The aim of this study is to determine the most beneficial radiation treatment technique for pediatric patients with thoracic and abdominal neuroblastoma (NBL), through a dosimetric comparison between photon Volumetric Modulated Arc Therapy and proton Intensity-Modulated Proton Therapy treatment plans.

Materials and Methods: A retrospective analysis was conducted on a multicentre case series of 19 patients with thoracic and/or abdominal NBL who underwent radiation therapy, following the recommendations of the European protocol for high-risk NBL (HR-NBL2/SIOPEN). The prescribed dose was 21.6 Gy in 12 fractions (1.8 Gy/fraction) delivered over the preoperative disease volume. The dose volume histograms were analyzed for each patient, and a Wilcoxon signed-rank test with a significance level of 0.01 was employed to assess statistical differences between the dosimetric parameters investigated. Two homogeneity indices (HI and $_{new}$HI) were compared to evaluate the uniformity in dose, delivered to the adjacent vertebrae (VBs_Adj).

Results: Both radiation techniques conform to the protocol regarding CTV/PTV coverage for every location. Proton therapy resulted in statistically significant dose sparing for the heart and lungs in supradiaphragmatic locations and for the contralateral kidney, liver, spleen, and bowel in subdiaphragmatic locations. For both techniques, sparing the non-adjacent vertebrae (VBs_NAdj) results more challenging, although promising results were obtained. Furthermore, the dose delivered to the VBs_Adj was not statistically different, in terms of homogeneity, for the 2 radiation techniques that both met the protocol's requirements.

Conclusion: This dosimetric analysis highlights the potential of protons to reduce radiation dose to healthy tissue. These findings apply to all the investigated patients, regardless of primary tumor location, making proton therapy a valuable option for the treatment of neuroblastoma. However, a multidisciplinary assessment of each case is essential to ensure the selection of the most effective and suitable treatment modality.

* Corresponding author. National Center for Oncological Hadrontherapy (CNAO), Via E. Borloni, 1, 27100 Pavia, Italy.
E-mail address: alfredo.mirandola@cnao.it (A. Mirandola).
https://orcid.org/0000-0003-2427-2329.

https://doi.org/10.1016/j.ijpt.2024.100100
Received 21 December 2023; Received in revised form 15 March 2024; Accepted 23 April 2024

Introduction

Neuroblastoma (NBL) is an embryonal solid tumor originating from neural crest cells in the sympathetic nervous system. Despite its rarity, it is the most common extracranial solid tumor in children, accounting for 7% to 8% of all pediatric tumors.[1] The average age at diagnosis is around 2 years.[2]

NBL typically arises from the adrenal medulla and less commonly from sympathetic ganglia elsewhere in the retroperitoneum or thorax. Advancements in treatment modalities have significantly improved the survival rates for high-risk NBL (HR-NBL) by up to 50%. Therefore, greater attention is now given to long-term side effects.

This study presents a retrospective analysis of a cohort of 19 patients with thoracic and/or abdominal diseases. The primary objective is to determine the most favorable technique for young patients through a dosimetric evaluation between photon and proton radiation therapy. It is progressively becoming required, in fact, to establish multidisciplinary standards that can help in selecting the most appropriate radiation therapy treatment, thereby optimizing health care resources at a national level.

In addition, the identification of criteria based on radiological image analysis, taking into account the anatomical location of the lesion and its relationships with the surrounding organs, may obviate the need for systematic dosimetric comparisons between photon and proton radiation therapy.

For this comparison, we have adopted the criteria outlined in the new European protocol for high-risk NBLs (HR-NBL2/SIOPEN—High-Risk Neuroblastoma Study 2 of SIOP-Europe-Neuroblastoma). The HR-NBL2/SIOPEN establishes a dose of 21.6 Gy in 12 fractions (1.8 Gy/fraction) at the preoperative tumor bed for patients who have undergone radical tumor resection. Randomization was planned for patients with macroscopic residual disease after high-dose chemotherapy and surgery. Arm one received 21.6 Gy at the preoperative tumor bed, while arm 2 received the same treatment, plus an additional 14.4 Gy boost in 8 fractions at the residual disease site. This study looked at the 21.6 Gy dose prescription, with the possibility of future investigations up to 36 Gy.

In addition, the protocol also focuses on reducing skeletal growth sequelae and improving the quality of life (QoL) for long-term survivors. Notably, in the planning optimization, now both vertebral dose gradient and homogeneous dose distribution within the vertebrae adjacent to the target volume should be included, as recommended in ref.[3] In particular, homogeneous dose distribution to VBs_Adj is recommended for children who have not yet reached pubertal growth spurt. A left/right and antero-posterior gradient shall be kept under 5 Gy (3 Gy) for children aged > 2 (< 2) years, following the protocol recommendations. Conversely, the dose at 5% of the volume ($D_{5\%}$) of the VBs_NAdj, both superior (S) and inferior (I), shall be kept under 15 Gy (10 Gy) for children aged > 2 (< 2) years.

Materials and methods

Patient characteristics

We conducted a retrospective multicenter analysis of a case series of 19 patients (14 males, and 5 females) diagnosed with NBL who underwent to radiation therapy at the National Centre for Oncological Hadrontherapy (CNAO) in Pavia, at the Fondazione IRCCS Istituto Nazionale Tumori in Milan and at the IRCCS Ospedale Policlinico San Martino in Genoa. The median age at the start of radiation therapy was 41 months. Written informed consent was obtained from all the patients or their legal guardians. All patient data has been collected under internal review board-approved protocol.

The primary tumor was located as a subdiaphragmatic disease in 7 (37%) patients, supradiaphragmatic disease in 5 (26%) patients, and with involvement both above and below the diaphragm in 7 (37%) patients. In addition, the study found that 7 (37%) patients had well-lateralized (paramedian) disease and 5 (26%) had lateralized disease with extension beyond half of the vertebral body (paramedian and median); 4 (21%) patients had further extension beyond the vertebral body with contralateral invasion, while only 3 (16%) had a central (median) localization. The CTV volumes ranged from 27.2 to 655.6 cc, with an average of 185.7 cc.

All patients underwent computed tomography (CT) simulations in the center they were referred to.

The definition of target volumes was based on CT and magnetic resonance imaging studies performed at the end of induction chemotherapy but before surgery. The GTV includes the extent of preoperative disease and persistently enlarged lymph nodes and is then modified on the CT scan obtained during simulation to exclude healthy organs that have been displaced by the tumor mass but have now returned to their original position. The CTV was obtained by expanding the GTV by 5 mm to include areas of possible microscopic disease spread, excluding anatomical barriers. The CTV should also encompass all areas of microscopic disease as indicated by the surgical report and histopathological examination. The PTV was obtained by expanding the CTV by 5 to 10 mm, with the expansion range varying depending on the facility clinical practice. CT scans were acquired with a slice thickness of 2 mm in 12 cases, and 5 mm in 7 cases.

Following the protocol's indication, we designated VBs_Adj as the vertebrae at the level of the PTV/CTV that cannot be adequately spared ($<$ 10-15 Gy) and require uniform irradiation, in accordance with the European Society for Paediatric Oncology (SIOPE) radiotherapy working group guidelines.[3] VBs_NAdj_S and VBs_NAdj_I were defined as the vertebrae cranial and caudal to VBs_Adj, respectively. The VBs_Adj were not included within the target volume but were irradiated homogeneously, fulfilling the required dose gradient. In the protocol, the definition of adjacent vertebra (VBs_Adj) is left to the discretion of the radiation oncologist. However, it is generally indicated if there is PTV overlap or within 1 cm on 2 or more slices, in order to achieve sufficient dose sparing ($D_{5\%} < 10$ Gy for children under 2 years and < 15 Gy for children > 2 years). However, this is in contrast with the recommendation to minimize the number of irradiated vertebral bodies in patients under 6 years of age (ideally to no more than 7).

Plan optimization

Protons

Proton plans were optimized with the Intensity-Modulated Proton Therapy (IMPT) technique using active Pencil Beam Scanning. For this planning study, we adopted the treatment planning system (TPS) proton beam settings routinely employed at CNAO in clinical practice.[4] However, the protocol simultaneously recommends a steep dose gradient for the VBs_NAdj and a high homogeneity for the VBs_Adj. To meet these requests, we used a smaller transverse spot distance (2 mm) for planning, needed to achieve a higher dose modulation. In case a single posterior beam is used, for simple cases (mostly thoracic), a higher modulation can be reached by using a 1 mm spot distance. A coarser spot distance (3 mm) would result in poor plan modulation. Therefore, to achieve the requested steep gradients while still maintaining high conformity to VBs_Adj and the target, a lower value is necessary. Conversely, if 2 or 3 fields are adopted, the spot grid could be coarser because the gradient zones could be targeted by particles arriving from multiple directions. Although a proton rotating gantry is currently unavailable at the CNAO facility, one of the operational treatment rooms is equipped with both horizontal and vertical beamlines, together with a 6-degree-of-freedom isocentric robotic couch, thus allowing several possible beam entrances. For this study, the proton plans were optimized for both fixed beam and gantry geometries. Fixed beam-based plans typically employed a posterior field, while a lateral (less weighted) field, passing through the liver for robustness, was added typically for abdominal sites when needed. Two

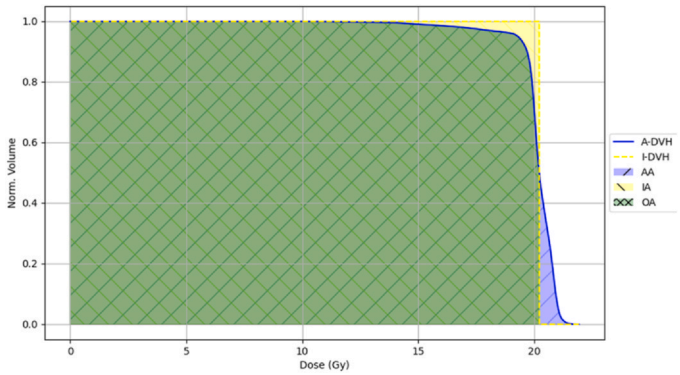

Figure 1. IA, in yellow, represents the area under the I-DVH curve; AA, in blue, represents the area under the A-DVH curve; OA, in green, is the overlapping area between IA and AA.

posterior fields, separated by 30 to 40 degrees, instead of a posterior beam only, could be employed for the gantry geometry. Other beam entrances were adopted, even passing through the liver for abdominal lesions, when needed. RayStation 11B (Raysearch Laboratories, Stockholm, Sweden) TPS with proton Pencil Beam Scanning Monte Carlo dose engine (Ion Monte Carlo v5.3) was employed for optimizing the plans.

To achieve the coverage goals for CTVs, a robust planning strategy based on min-max optimization[5,6] was applied, taking into account both setup errors (± 3 mm) and beam range uncertainties (± 3%).

When available (3 out of 19 cases), gated CT scans were retrospectively reconstructed, and the respiratory cycle was divided into 6 different phase end-expiration, end-inspiration, 30% inspiration, 30% expiration, 50% inspiration, and 50% expiration, similarly to ref.[7] For patients who actually received proton treatment, the prone position and the thermoplastic immobilization mask adopted, reduced the effect of the motion. In addition, the respiratory movement is even more mitigated when anesthesia is performed. Therefore, the optimization strategy in these 3 cases was to plan at the end-expiration phase, incorporating the end-inspiration into the robust optimization. The calculated plans were robust in both the end-expiration and end-inspiration phases, allowing the patients' treatments to be delivered in free-breathing mode since both CTV coverage and OARs sparing fulfill the clinical requirements with negligible changes.

Photons

Photon treatment plans were optimized using Volumetric Modulated Arc Therapy (VMAT). Depending on the complexity of the target volume (PTV), 2 to 4 coplanar arcs were used, counterclockwise and clockwise with the same starting and end angle. If the arc dimension is higher than 10 to 15 cm in the lateral direction, each arc is splitted and a field overlap of 2 cm is maintained.

For radiation treatment, Varian TrueBeam or DHX linear accelerators, equipped with a multileaf Millennium collimator consisting of 120 leaves, were used. Eclipse (Varian Medical Systems, Palo Alto, California) TPS for photon plans were adopted: version 13.5 in Genoa and version 15 in Milan. Photon VMAT Optimization version 13.5.35 and 15.6 algorithms were used for plan optimization. Dose calculations were performed using the analytical anisotropic algorithm, with a calculation grid size of at least 0.25 cm.

Plan analysis and comparison

For the evaluation of target coverage, as specified in the protocol, we focused exclusively on the CTVs, since the PTVs were not included in the IMPT optimization process.

Nonetheless, an evaluation of the proton plan robustness was performed for each case. The latter was conducted by examining 42 different scenarios based on the following robustness parameters: ± 3 mm for setup errors and ± 3% for range uncertainties.

Statistical significance was tested using the Wilcoxon signed-rank test with a significance level (*P*-value) of 0.01 to verify the null hypothesis H_0 that 2 investigated dosimetric parameters are equal for proton and photon plans (H_0: ${}_{p}$DVH = ${}_{ph}$DVH).

Finally, the protocol underlines the need for homogeneity in the adjacent vertebral region, with limitations of an anterior/posterior and left/right gradient. Less than 5 Gy for children aged > 2 years and 3 Gy for those aged < 2 years are required. In order to assess the homogeneity, surrogate metrics, based on the more widely used homogeneity indices, were evaluated.

In particular, the following 2 homogeneity indices were investigated.

The first index is the Homogeneity Index (HI) as defined in International Commission on Radiation Units & Measurements Report 83.[8]

$$HI = \frac{(D_{2\%} - D_{98\%})}{D_{50\%}}$$

The second index is the ${}_{new}$HI as defined by Yan et al[9]

$$HI = \frac{OA^2}{(IA*AA)}$$

where IA stands for the region below the ideal dose volume histogram (DVH) curve where the entire volume of the VBs_Adj is expected to achieve the $D_{50\%}$ of the achieved DVH, AA represents the area under the A-DVH curve and OA is the overlapping area between IA and AA.

High homogeneity is indicated by values approaching 0 and 1, for HI and ${}_{new}$HI indices, respectively. The Figure 1 graphically explains the abovementioned quantities for a real case.

Results

For photons, minor deviations in PTV coverage ($D_{98\%}$ < 95%) were detected in 16% of the 19 patients, with no major deviations. Conversely, there were no protocol deviations for proton plans.

Regarding organs at risk (OARs), the single kidney dose limit ($D_{10\%}$ ≤ 15 Gy) was achieved neither for proton nor for photon technique. 11 patients for protons and 10 for photons received, in fact, a dose higher than 15 Gy. However, $D_{50\%}$ was below 15 Gy for each case and for both techniques, ensuring preserved kidney functionality.

No protocol deviations were detected for the combined kidneys, combined lungs, bowel, spinal cord, and heart, as the dose constraints for both proton and photon plans were not exceeding the dose limits.

A few deviations were found for the spleen, with 2 cases for photons and 1 for protons in abdominal cases.

Compliance with the strict dose constraints for VBs_NAdj ($D_{5\%}$ < 10 Gy, for children under the age of 2 years) was a challenge. Only 6 cases (all photon plans) met the protocol requirements. However, these results are heavily influenced by the low resolution of the CT scans used

Table 1
Targets and OARs dosimetric values for proton nominal scenario (p) and photon (ph) plans together with the results of the Wilcoxon statistical test (*P*-value).

ROI	Dose statistic	Mean (p)	Range (p)	Mean (ph)	Range (ph)	*P*-value
CTV	$D_{99\%}$	20.9	20.10-21.25	21.07	20.20-21.29	< .01
	$D_{98\%}$	21.02	20.22-21.30	21.15	20.30-21.37	
	$D_{95\%}$	21.19	20.41-21.38	21.25	20.40-21.38	
PTV	$D_{98\%}$	-	-	20.74	19.97-21.21	-
	$D_{95\%}$	-	-	21.03	20.20-21.40	
Spinal cord	$D_{0.01cc}$	20.88	19.03-22.55	20.76	17.27-21.90	.39
VBs_NAdj_S	$D_{5\%}$	11.67	10.09-13.56	11.68	4.73-15.72	.44
VBs_NAdj_I	$D_{5\%}$	11.95	9.75-15.57	11.94	4.53-17.32	.4
Heart (th)	$D_{50\%}$	0.07	< 0.00-0.39	5.28	0.47-8.32	< .01
	$D_{10\%}$	7.34	< 0.01-13.16	10.98	3.49-17.59	< .01
Heart (ab)	$D_{50\%}$	0.09	< 0.01-0.59	2.26	0.20-7.24	< .01
	$D_{10\%}$	4.7	< 0.01-17.81	7.02	0.35-16.35	< .01
Kidney_omo (th)	$D_{50\%}$	2.2	0.10-11.98	4.01	0.88-7.82	.05
	$D_{10\%}$	11.84	6.96-20.21	11.59	6.21-19.54	.26
Kidney_omo (ab)	$D_{50\%}$	8.21	3.99-13.19	11.4	3.19-20.64	< .01
	$D_{10\%}$	17.23	17.15-21.79	18.51	20.23-21.85	.02
Kidney_con (th)	$D_{50\%}$	1.36	0.05-7.83	3.2	0.71-6.99	< .01
	$D_{10\%}$	7.19	1.05-19.32	7.5	3.52-16.66	.31
Kidney_con (ab)	$D_{50\%}$	1.58	0.05-4.08	3.7	1.83-5.30	< .01
	$D_{10\%}$	9.94	3.56-18.20	8.43	4.23-12.52	.35
Kidneys (th)	$D_{50\%}$	1.72	0.07-9.89	3.72	0.80-7.10	< .01
	$D_{30\%}$	3.81	0.19-16.12	5.21	1.38-9.26	.1
Kidneys (ab)	$D_{50\%}$	3.53	< 0.01-9.28	6.89	2.10-12.54	< .01
	$D_{30\%}$	8.19	< 0.01-14.49	11.16	3.83-19.31	< .01
Lungs (th)	$D_{50\%}$	0.38	0.10-1.27	7.58	0.31-9.15	< .01
	$D_{25\%}$	3.84	0.15-11.30	8.53	1.86-14.50	< .01
Lungs (ab)	$D_{50\%}$	0.07	< 0.00-0.20	3.51	0.14-10.90	< .01
	$D_{25\%}$	0.58	< 0.01-1.96	4.21	0.22-10.74	< .01
Liver (th)	$D_{50\%}$	0.11	< 0.01-0.55	6.34	7.04-8.60	< .01
Liver (ab)	$D_{50\%}$	0.54	0.01-2.84	7.01	6.72-9.42	< .01
Spc bowel (th)	$D_{100\%}$	< 0.00	< 0.00	0.02	< 0.01-0.11	< .01
	$D_{50\%}$	< 0.00	< 0.00	1.65	< 0.01-7.75	
	$D_{10\%}$	1.33	< 0.01-9.30	4.31	< 0.01-16.55	
Spc bowel (ab)	$D_{100\%}$	< 0.00	< 0.00	0.32	< 0.01-0.60	< .01
	$D_{50\%}$	3.56	< 0.01-16.61	9.22	0.31-19.09	
	$D_{10\%}$	15.61	< 0.01-21.83	17.46	3.91-21.86	
Spleen (th)	$D_{50\%}$	0.19	< 0.01-0.76	3.69	< 0.00-8.29	< .01
Spleen (ab)	$D_{50\%}$	3.75	< 0.01-12.77	8.84	1.23-18.50	< .01

for these cases. Five of these 6 cases were calculated on a coarse simulation CT, with a slice thickness of 5 mm. The latter is unacceptable, according to current contouring and planning standards, especially when a steep dose gradient is required, as in this case. Furthermore for 18 out of 19 proton plans 10 Gy < $D_{5\%}$ < 15 Gy, with only one case with $D_{5\%}$ higher than 15 Gy. In 7 cases the photon plans showed 10 Gy < $D_{5\%}$ < 15 Gy and 6 cases with $D_{5\%}$ higher than 15 Gy.

Beyond the compliance to the protocol, data extracted from the DVH analysis were also used to compare proton and photon plans using the Wilcoxon signed-rank test with a *P*-value of .01. Table 1 below

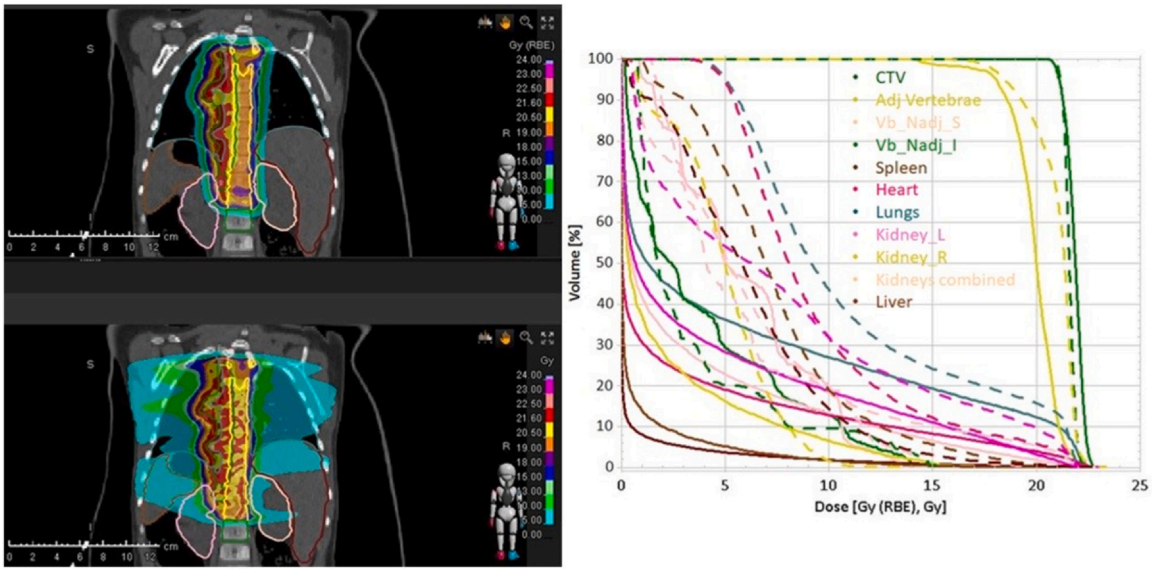

Figure 2. Coronal view of a proton (upper left panel) and photon plan (lower left panel). Right panel: solid and dashed lines represent proton nominal and photon plan DVHs, respectively. Abbreviation: DVHs, dose volume histograms.

summarizes both the dosimetric values for proton (nominal scenario) and photon plans and the results of the statistical test, with the *P*-value.

A detailed comparison, based on the dosimetric parameters reported in Table 1, between fixed beam and gantry proton plans was performed for 7 out of the 19 patients. According to Table 1s in the Supplementary Materials, no significant differences were found. The remaining 12 patients had beam arrangements that were clearly either 1, 2, or 3 cardinal beams, thereby avoiding the need to use the gantry. Comparable results were achieved, with and without the use of a gantry in terms of target coverage, both in the nominal plan and in the robustness evaluation (± 3 mm, ± 3%), and OARs sparing. Conversely, the use of a gantry could result in an increase in low doses to the kidneys and VBs_NAdj, although still in compliance with the protocol.

For this reason, without loss of generality, data for protons reported in Table 1 refer to fixed beam geometry only. As the location of the targets affects the dose delivered to some OARs, the dosimetric results were divided into 2 main anatomical categories, the thoracic (th) and abdominal (ab) ones.

Figure 2 illustrates a plan comparison example for a thoraco-abdominal NBL: low doses are clearly minimized with IMPT with respect to VMAT.

Regarding the VBs_Adj, both techniques ensure protocol compliance, without any deviations. The requested left/right and anterior/posterior gradient (5 Gy or 3 Gy for younger children), in fact, is fulfilled since the VBs_Adj were uniformly irradiated in all 19 cases, regardless of the radiation technique used. Furthermore, the HI was 0.269 ± 0.056 and 0.241 ± 0.075 for protons and photons, respectively. The $_{new}$HI was 0.965 ± 0.010 and 0.952 ± 0.017, for protons and photons respectively. The Wilcoxon test showed no statistical differences between the 2 techniques. As an example, Figure 4 shows the latero-lateral dose profiles of a VBs_Adj, for both radiation techniques.

Before the recent clinical introduction of the dose homogeneity to the vertebral body along the lateral-lateral and antero-posterior directions, the vertebral body was intended as an organ at risk and spared as much as possible. Figure 4 shows a comparison between a proton treatment plan with the intentional homogeneous coverage of the VBs_Adj (on the left) and a treatment plan that spares it. The lateral dose profile shows the dramatic changes introduced by the concept of dose homogeneity within the VBs_Adj.

Robust evaluation for proton plans

In order to give a general overview of the 42 robustness scenario within the investigated patient cohort, the following Table 2, for fixed beam geometry, has been reported. The third column shows the percentage of the scenarios, averaged on the patient cohort, passing the dosimetric requirement reported in the second column. The fourth column reports, for each parameter, the worst patient case within the cohort. The collected results show that the nominal plan still maintains satisfactory robustness across the perturbed scenarios.

In addition, the robust analysis of the CTVs coverage showed that $D_{95\%}$ is higher than 95% of the dose prescription in more than 98% of the robustness scenarios, for all the patients analyzed. Although not strictly requested by the protocol, a high homogeneity within the CTV is achieved:

HI < 0.12 for all the proton plans (nominal scenario) and $D_{98\%}/D_{2\%}$ is higher than 0.9 for at least 95% of the robustness scenario, for all the investigated patients.

As far as the VBs_Adj is concerned, the anterior-posterior and latero-lateral dose profiles along the vertebral body still fulfill the protocol's requirements (dose gradient less than 5 Gy or 3 Gy) for whatever robustness scenario, for all the investigated patients.

Discussions

Regarding CTV coverage, the results obtained and reported in Table 1 are consistent with Hill-Kayser et al.[10] The study analyzed a set

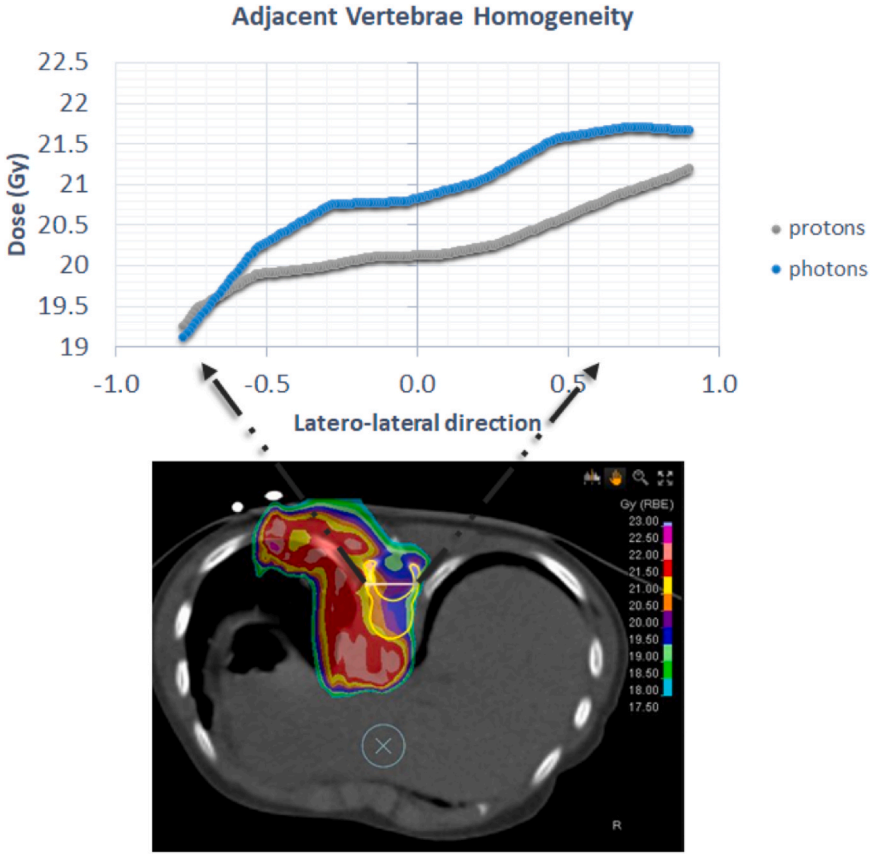

Figure 3. Adjacent vertebrae homogeneity: lateral dose profile.

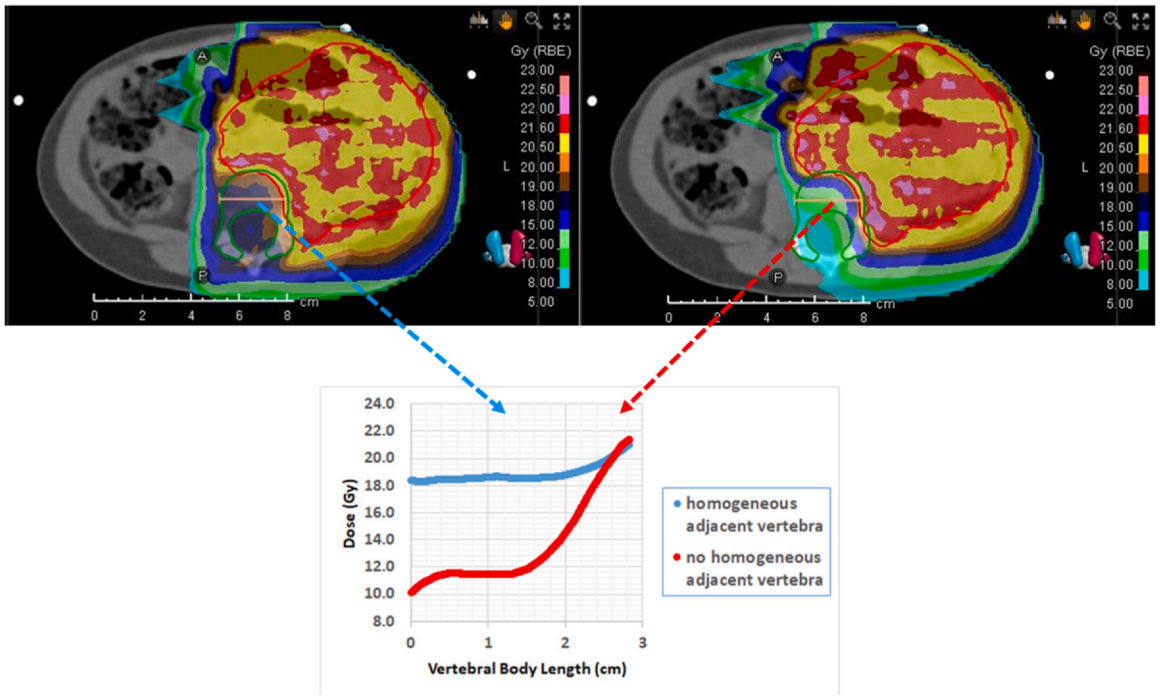

Figure 4. Adjacent Vertebrae, proton plan examples: homogeneous intentional irradiation (left panel and blue latero-lateral dose profile); intentional sparing of the vertebra (right panel and red latero-lateral dose profile).

Table 2
Robustness analysis for proton plans: the second column reports the dosimetric requirements, the third column shows the percentage of the scenarios, averaged on the patient cohort, passing the dosimetric requirement.

ROI	Dose parameter	Passed ± 1 std (%)	Minimum passed scenario in the cohort (%)
CTV	$D_{95\%}$ > 95%	96.7 ± 3.8	88
Spleen	$D_{50\%}$ < 10 Gy	98.0 ± 6.2	79
Heart	$D_{50\%}$ < 15 Gy	100; all cases	100
Lungs	$D_{25\%}$ < 15 Gy	100; all cases	100
	$D_{50\%}$ < 12 Gy	100; all cases	100
Liver	$D_{50\%}$ < 21 Gy	100; all cases	100
Kidneys	$D_{50\%}$ < 15 Gy	100; all cases	100
	$D_{30\%}$ < 20 Gy	100; all cases	100
Kidney Con.	$D_{50\%}$ < 15 Gy	100; all cases	100
	$D_{10\%}$ < 15 Gy	89.4 ± 17.3	52
Kidney Omo.	$D_{50\%}$ < 15 Gy	99.2 ± 2.2	93
VBs_NAdj_S	$D_{5\%}$ < 15 Gy	87.0 ± 11.2	64
VBs_NAdj_I	$D_{5\%}$ < 15 Gy	80.6 ± 14.9	53

The fourth column reports the worst patient case within the cohort.

of HR-NBL patients, in which 95% of the CTV received a median dose of 99% for proton therapy (PT) and 100% for IMRT. Our investigation confirmed the overlap in target volume coverage between photon and proton techniques.

Furthermore, our study demonstrated that proton planning achieves significant dose-sparing across a wide range of OARs. This advantage is not influenced by the location of the primary tumor, whether in the abdominal or thoracic region, confirming the benefits of proton planning for these patients.

Our results show that when PT is delivered to the subdiaphragmatic site, the median doses to the liver and spleen, as well as the median, minimum, and $D_{10\%}$ doses to the peritoneal cavity, are significantly reduced. These results are consistent with previous scientific reports confirming a significant reduction in $D_{50\%}$ and $D_{20\%}$ at the hepatic level when using PT.[10] It is important to highlight the importance of lower doses as they have been associated with hepatotoxicity in patients previously treated for abdominal Wilms' tumor. It is worth noting that among the relevant hepatic toxicities, veno-occlusive disease/sinusoidal obstruction syndrome is prevalent, which is characterized by damage to the endothelial cells of the liver sinusoids. Unfortunately, there are currently no specific dose limits to prevent veno-occlusive disease. However, it is suggested that the dose to the liver should be limited as much as possible while still ensuring adequate target coverage.[11,12]

With respect to kidney dose, although all dosimetric indicators generally show lower values for proton treatment plans, only the $D_{50\%}$ to the contralateral kidney and kidneys combined were significantly lower compared to the VMAT technique. Previous research also demonstrates a tendency for lower kidney dose, especially for the contralateral kidney, when using PT, even though this decrease was not statistically significant. Indeed, even when the disease was lateralized and the dose to the ipsilateral kidney was lower with photon radiation therapy, the overall advantage for both kidneys suggests the adoption of PT as the preferred option.[11,13]

A recent study has demonstrated the advantage of PT in terms of dose sparing in all the examined OARs for laterally located lesions. Instead, for median lesions, the benefit was significant only for the combined kidneys and liver.[14] In our analysis, we found that

paramedian lesions accounted for 37% of cases. Although we did not conduct a subanalysis based on the location of the disease, there was a statistically significant difference in the median dose to the contralateral kidney.

To minimize the dose to the kidneys, we recommend considering the complexity of assessing the risk of long-term complications, particularly when using nephrotoxic drugs concurrently. Priority should be given to preserving the remaining kidney in children who have undergone unilateral nephrectomy.[15]

It is important to highlight that neuroblastoma is usually located in the retroperitoneal compartment (9 patients out of 19 in our analysis) and often presents with large disease volumes. Proton therapy achieves a greater reduction of low doses to intraperitoneal structures compared to cases treated with craniospinal radiotherapy.

For supradiaphragmatic locations, we achieved significantly lower doses with PT for both the heart and lungs. Reducing radiation exposure to the heart, especially considering the young age of patients with NBL, is crucial since exposure to ionizing radiation, especially at a young age, is a significant risk factor for developing cardiovascular diseases in adulthood.[16]

In our case series, we also observed a statistically significant reduction in $D_{25\%}$ and mean doses for both lungs. The values were consistently below tolerance thresholds, confirming the advantage of PT in reducing pulmonary irradiation, as previously shown in dosimetric studies. This could represent a critical point in optimizing the post-therapy QoL[17] while the reduction in the volume of lung irradiated to low doses is crucial for long-term outcomes in patients with thoracic NBL.[18]

The analysis conducted on the vertebral bodies showed that PT could lower the risk of scoliosis and growth problems. This highlights the potential advantages of PT in pediatric patients. Recent literature suggests that including the entire vertebral body in the treatment field can limit radiation-induced growth deficits in children,[19,20] although the threshold beyond which alterations begin to occur is not yet precisely defined. Currently, it is recommended to irradiate the VBs-Adj at a dose of 18 to 20 Gy, beyond which the first measurable deficits are observed.[21] Dysmorphisms, particularly scoliosis, also represent a late sequel that develops many years after radiation treatment, especially in patients who have received doses exceeding 18 Gy or dose gradients within the vertebrae greater than 10 Gy.[22] Our analysis showed a $D_{50\%}$ at the level of VBs_Adj of 19.63 Gy for protons and 20.33 Gy for photons, respectively.

As mentioned in the result section, the VBs_NAdj constraints ($D_{5\%} < 10$GyE for patients aged < 2 years) were met for photons in 6 out of 19 cases. However, in 5 of these cases, the CT scan slice thickness was 5 millimeters, resulting in an imprecise definition of the interface between the vertebrae and a rough estimate of the dose to the bony structures. This introduces bias in the evaluation of the dose to VBs_NAdj. To avoid coarse and uncertain results, it is necessary to follow the protocol recommendation and perform the CT scan every 2 millimeters (however $\leq$ 3 mm).

To date, the clinical impact of these dosimetric advantages remains an open question that will only be answered in long-term follow-up studies. The observed dosimetric differences may potentially lead to clinical benefits such as reduced toxicity rates and improved QoL for survivors, making PT an attractive treatment option for pediatric patients with NBL.

It is important that range uncertainties in proton therapy are carefully managed. Unlike photons, 2 severe consequences can occur due to the potential shift of the proton sharp distal dose fall-off: underestimation of dose to the target or overdosage to the OARs distal to the beam direction.[23] Range uncertainties can arise from organ motion, setup and anatomical variations, dose calculation approximations, and biological considerations. To account for both setup errors and range uncertainties, robust planning optimization[24] is strongly recommended when using protons. Data reported in Table 2 shows how the proton plans keep high robustness for the CTV and the majority of the OARs across the 42 scenarios and for each patient, while the VBs_NAdj is the less robust OAR. This is due to the homogeneity imposed to the contiguous VBs_Adj that conflicts with the strict $D_{5\%} < 15$ Gy desired for the VBs_NAdj. Therefore the scenarios involving the superior-inferior shifts worsen the robustness statistic. For NBL diseases, both moving and emptying/filling regions such as the stomach, bowel, and duodenum are involved. Therefore, it is necessary to perform a re-evaluation CT scans during the treatment course, to recalculate the plan and minimize interfraction variations. In such cases, it is advisable to consider mitigation strategies such as breath-hold and respiratory gating, both during CT simulation and, if needed, during treatment. As previously mentioned, special attention should be addressed to the impact of organ motion, particularly in the context of proton plans. For the 3 evaluated patients, adding the 2 opposite respiratory phases in the robust calculation is sufficient to ensure both the CTV coverage and OARs sparing during free-breathing treatment. However, a patient-specific assessment in this regard is strongly recommended, and should not be dismissed outright during the treatment phase. In addition, patients with masks and in the prone position, particularly if they are under anesthesia, experience minimal OAR and tumor motion, especially for retroperitoneal lesions. For the thoracic site, a single proton posterior field was sufficient to meet the protocol's requests and the robustness criteria, even by recalculating plans on the re-evaluation CTs acquired during the course of treatment, when available. For the abdominal site, instead, 1 or 2 posterior and 1 lateral fields were used to achieve the same satisfactory results. While a rotating gantry may be beneficial in certain cases, it does not offer significant advantages for this patient cohort and prescription dose level. Confirmation of these findings for higher doses is necessary, particularly for the additional boost to 36 Gy, as the dose limit to the spinal cord may become a concern.

Conclusions

The dosimetric analysis clearly shows that PT has the potential to reduce radiation exposure to all the investigated OARs, especially those located in the thoraco-abdominal region. This advantage extends to all patients, regardless of the primary tumor site, making PT a valuable option for the treatment of NBL.

The introduction of well-defined multidisciplinary criteria, based on radiological image analysis and developed by experienced pediatric oncologists, pediatric surgeons, and radiation oncologists, is essential to identify the most appropriate radiation treatment for each patient. This approach could limit the need for systematic dosimetric comparisons between photon and PT, allowing for more effective patient allocation and resource optimization at the national level.

Author contributions

A.M., S.V. and F.Co. conceived of the presented idea. **A.M., S.V., and F.Co** developed the theory. **A.M., F.Ca, A.C., E.P., M.C., and S.M.** performed the computations. All authors verified the analytical methods and discussed the results and contributed to the final manuscript.

Declaration of Conflicts of Interest

The authors declare the following financial interests/personal relationships which may be considered as potential competing interests: Alfredo Mirandola reports administrative support, article publishing charges, equipment, drugs, or supplies, statistical analysis, travel, and writing assistance were provided by National Centre of Oncological Hadrontherapy. Alfredo Mirandola reports a relationship with the National Centre of Oncological Hadrontherapy that includes: employment. Alfredo Mirandola has patent issued to no. Nothing to add If there are other authors, they declare that they have no known competing

financial interests or personal relationships that could have appeared to influence the work reported in this paper.

Appendix A. Supporting information

Supplementary data associated with this article can be found in the online version at doi:10.1016/j.ijpt.2024.100100.

References

1. Park JR, Hogarty MD, Bagatell R, et al. Neuroblastoma: epidemiology. In: Blaney SM, Helman LJ, Adamson PC, eds. *Pizzo and Poplack's Pediatric Oncology*. 8th ed. Philadelphia: Wolters Kluwer; 2021:647.1.
2. Qiu B, Matthay KK. Advancing therapy for neuroblastoma. *Nat Rev Clin Oncol.* 2022;19(8):515–533. https://doi.org/10.1038/s41571-022-00643-z
3. Hoeben BA, Carrie C, Timmermann B, et al. Management of vertebral radiotherapy dose in paediatric patients with cancer: consensus recommendations from the SIOPE radiotherapy working group. *Lancet Oncol.* 2019;20(3):155–166. https://doi.org/10.1016/S1470-2045(19)30034-8 PMID: 30842059.
4. Mirandola A, Molinelli S, Freixas GV, et al. Dosimetric commissioning and quality assurance of scanned ion beams at the italian national center for oncological hadrontherapy. *Med Phys.* 2015;42:5287–5300. https://doi.org/10.1118/1.4928397
5. Fredriksson A, Forsgren A, Hårdemark B. Minimax optimization for handling range and setup uncertainties in proton therapy. *Med Phys.* 2011;38:1672–1684. https://doi.org/10.1118/1.3556559
6. Stuschke M, Kaiser A, Pöttgen C, Lübcke W, Farr J. Potentials of robust intensity modulated scanning proton plans for locally advanced lung cancer in comparison to intensity modulated photon plans. *Radiother Oncol.* 2012;104:45–51. https://doi.org/10.1016/j.radonc.2012.03.017
7. Molinelli S, Vai A, Russo S, et al. The role of multiple anatomical scenarios in plan optimization for carbon ion radiotherapy of pancreatic cancer. *Radiother Oncol.* 2022;176:1–8. https://doi.org/10.1016/j.radonc.2022.09.005
8. International Commission on Radiation Units and Measurements ICRU report 83 prescribing, recording, and reporting photon-beam intensity-modulated radiation therapy (IMRT). Journal of the ICRU, 2010; 10(1).
9. Yan L, Xu Y, Chen X, Xie X, Liang B, Dai J. A new homogeneity index definition for evaluation of radiotherapy plans. *J Appl Clin Med Phys.* 2019;20:50–56. https://doi.org/10.1002/acm2.12739
10. Hill-Kayser C, Tochner Z, Both S. Proton versus photon radiation therapy for patients with high-risk neuroblastoma: the need for a customized approach. *Pediatr Blood Cancer.* 2013;60(10):1606–1611. https://doi.org/10.1002/pbc.24606
11. Kandula S, Sutter A, Prabhu RS. Reassessing dose constraints of organs at risk in children with abdominal neuroblastoma treated with definitive radiation therapy: a correlation with late toxicity. *Pediatr Blood Cancer.* 2015;62(6):970–975. https://doi.org/10.1002/p
12. Horn B, Reiss U, Matthay K. Veno-occlusive disease of the liver in children with solid tumors undergoing autologous hematopoietic progenitor cell transplantation: a high incidence in patients with neuroblastoma. *Bone Marrow Transplant.* 2002;29:409–415.
13. Jouglar E, Wagner A, Delpon G. Can we spare the pancreas and other abdominal organs at risk? A comparison of conformal radiotherapy, helical tomotherapy and proton beam therapy in pediatric irradiation. *PLoS One.* 2016;10(11):e0164643. https://doi.org/10.1371/jou
14. Lim PS, Rompokos V, Bizzocchi N. Pencil beam scanning proton therapy case selection for paediatric abdominal neuroblastoma: effects of tumour location and bowel gas. *Clin Oncol.* 2021;33(3):132–142. https://doi.org/10.1016/j.clon.2020.08.012
15. Jazmati D, Brualla L, Littooij AS. Overcoming inter-observer planning variability in target volume contouring and dose planning for high-risk neuroblastoma—a European multicenter effort of the SIOPEN radiotherapy committee. *Radiother Oncol.* 2023;181:109464.
16. van Nimwegen FA, Schaapveld M, Cutter DJ, et al. Radiation dose-response relationship for risk of coronary heart disease in survivors of Hodgkin lymphoma. *J Clin Oncol.* 2016;34:235–243. https://doi.org/10.1200/JCO.2
17. Shi A, Zhu G, Wu H. Analysis of clinical and dosimetric factors associated with severe acute radiation pneumonitis in patients with locally advanced non-small cell lung cancer treated with concurrent chemotherapy and intensity-modulated radiotherapy. *Radiat Oncol.* 2010;5:35. https://doi.org/10.1186/1748-717X-5-35
18. Bölling T, Dirksen U, Ranft A. Radiation toxicity following busulfan/melphalan high-dose chemotherapy in the EURO-EWING-99-trial: review of GPOH data. *Strahlenther Onkol.* 2009;185:21–22. https://doi.org/10.1007/s00066-009-1009-9
19. Ding Y-Y, Panzer J, Maris JM. Transverse myelitis as an unexpected complication following treatment with dinutuximab in pediatric patients with high-risk neuroblastoma: a case series. *Pediatr Blood Cancer.* 2018;65. https://doi.org/10.1002/pbc.26732
20. Dörr W, Kallfels S, Herrmann T. Late bone and soft tissue sequelae of childhood radiotherapy. Relevance of treatment age and radiation dose in 146 children treated between 1970 and 1997. *Strahlenther Onkol.* 2013;189:529–534.
21. Ng LW, Wong KK, Ally Wu CL. Dose sculpting intensity modulated radiation therapy for vertebral body sparing in children with neuroblastoma. *Int J Radiat Oncol Biol Phys.* 2018;101(3):550–557. https://doi.org/10.1016/j.ijrobp.2018.02.015
22. Riseborough EJ, Grabias SL, Burton RI. Skeletal alterations following irradiation for Wilms' tumor: with particular reference to scoliosis and kyphosis. *J Bone Jt Surg Am.* 1976;58:526–536.
23. Paganetti H. Range uncertainties in proton therapy and the role of Monte Carlo simulations. *Phys Med Biol.* 2012;57(11):99–117. https://doi.org/10.1088/0031-9155/57/11/R99.71
24. Unkelbach J, Paganetti H. Robust proton treatment planning: physical and biological optimization. *Semin Radiat Oncol.* 2018;28(2):88–96. https://doi.org/10.1016/j.semradonc.2017.11.005